



Analysis of Eddy Current Density using ANSYS MAXWELL Software

Muhammad Nassier Ahamad¹, Siti Amely Jumaat^{1,2*}

¹Faculty of Electrical and Electronics Engineering,
 Universti Tun Hussein Onn Malaysia, 86400, Batu Pahat, Johor, MALAYSIA

²Green and Sustainable Energy Focus Group (GSEnergy), Faculty of Electrical and Electronics Engineering,
 Universti Tun Hussein Onn Malaysia, 86400, Batu Pahat, Johor, MALAYSIA

*Corresponding Author

DOI: <https://doi.org/10.30880/jeva.2020.01.02.005>

Received 04 August 2020; Accepted 21 December 2020; Available online 28 December 2020

Abstract: This paper presents the simulation of eddy current density I_{CD} over the non-ferrous materials. Correlation between I_{CD} that circulates in non-ferrous magnetic material can stimulate the suspension force. Some simulation have been done using Finite Element Method (FEM) that is provided by ANSYS Maxwell simulator software in order to illustrate the formation of I_{CD} . The 3-dimensional shape of current-carrying coil suspended 1 cm over non-ferrous conductor is sketched up to emphasize or illustrate the existence of vertical magnetic forces. From simulation, the productivity of I_{CD} clearly appears on the top of conductor's surface whose interpretation comes from a current-carrying coil reaction. The causality is dependent on conductor properties, input frequency of current AC source, and conductor thickness that influence the amount of I_{CD} . The results show that the maximum I_{CD} is increased to 20 KA/m² when the thickness and the frequency are increased to 9 cm and 60 Hz respectively for the copper material. As a conclusion, the higher thickness and frequency of AC current will encourage the formation of I_{CD} . It can also be concluded that the high magnetization enable for more I_{CD} conduction.

Keywords: Eddy Current, Finite Element Method, Magnetic Levitation

1. Introduction

In the area of globalization, land and rail transportation are still relevant and have been used as containerization, intermodal transportation and locomibility of passengers around the globe. Discriminatory as old school transportation, the train sector has been evolved drastically in terms of manufacture and technology production without ignoring the safety and comfortability of passengers, traveling time rapidity, and reliability [1, 2]. Therefore, an advanced magnetic levitation (Maglev) system has been chosen as latest technology to interchange and upgrading the conventional railway train services and facilities. In no doubt, this beneficial system practically has denied an undesirable phenomenon like a derailment, energy loses by friction, and environmental impact caused by carbon dioxide emission [2]. Purposely to against the existence of undesirable friction between train and guideway, the Maglev system dependably relies on suspension force whether by attractive or repulsive force. Both forces are created by electromagnetic suspension (EMS) or electrodynamic suspension (EDS) method. Similarly, to the EDS concept, the repulsive force possibility can be done from the composition of eddy current levitation and diamagnetic levitation technique. Eventhough these technique produces weaker repulsive force than others, it still refute the Earnshaw's theorem related to levitation

stabilization [3, 4]. In industrial application, the eddy current diamagnetic levitation is still unaffordable to replace the latest technology due to its insufficient force productivity. Application of eddy current is more on the braking system, heating and melting process, and non-destructive testing [5, 6, 7]. In few decades to come, the research and development of eddy current levitation are never-ending toward amplifying the repulsion force.

Paper [8] describes the example of electromagnetic suspension and the levitation method. The available method such as levitation using diamagnetic materials and levitation using eddy current are described clearly by the author. This paper also explains the basic principle related to suspension with some examples of application. Paper [9] describes the fundamental of Eddy current levitation with a simple demonstration. The copper coil was excited with AC nominal current at 60 Hz and it enable it to levitate over aluminium plate. The levitation concept is based on three basic principles: Ampere Law, Faraday Law and Lorentz Law. By evaluating a simple equivalent electrical model, the author enables to identify a basic formula related to terminal inductance and energy usage. They also published a reliable formula to determine a lift-off power, levitation height, and suspension resonant frequency. Meanwhile, paper [10] describes the theory of eddy current with simple testing. Eddy current is fundamentally related to induced voltage that is influenced by the inductor. When the eddy current is applied on the creak plate, the impedance will be effected. Other than that, this paper also manifests some factors that enhance or mitigate the eddy current development on certain material. Paper [11] describes the summarized process of magnetization at the microscopic level. This paper also distinguishes the characteristic of diamagnetism, magnetism, and ferromagnetism in terms of molecular and atomic structure. Paper [12] conducts the simulation model using ANSYS Maxwell in order to find out the density of eddy current. Besides that, the impedance value of the circuit will impact the lift-off result related to mutual inductance between equivalent circuits of the coil with the conductor circuit. In addition, paper [4] describes the properties of diamagnetic, paramagnetic and ferromagnetic.

The main purpose of this paper are to design the copper (diamagnetic) and aluminium (paramagnetic) eddy current levitation model, measure the value of I_{CD} that is induced in the plate and analyze the relationship between I_{CD} inductions correlated to material thickness, and frequency source.

2.0 Electromagnetic Field Induction.

From electromagnetism theory, the interaction between the motions of electric charge moves throughout the infinitesimal region of a current-element conductor will form the insidious electromagnetic field (EMF). Similarity to magnetic behaviour, the EMF from a time-varying AC that exhibits from the exciter coil is verified as magnetic field lines B which indicates the direction of the magnetic force. These lines travel alike magnetic dipole along North-South pole in the form of a concentric circle [13]. The lines are strengthened with some magnetic field strength H and the strength is weaker when it is further away from the coil. The H-field that is discharged from the coil is proportional to the direction of current coil. H-field can be illustrated using the right-hand grip rule theorem to find out the circular direction while its strength along the central axis can be evaluated using Biot-Savart as shown in Fig. 1.

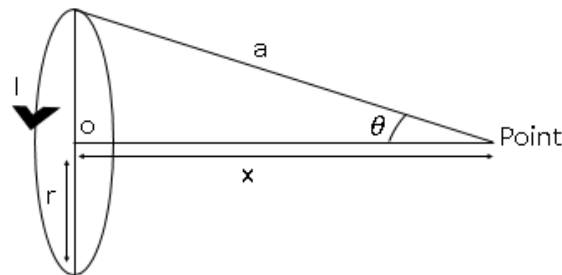


Fig. 1 - Current-carrying coil [13]

$$H_{\text{along central axis}} = \frac{\mu_0 2\pi N I r^2}{4\pi (x^2 + r^2)^{\frac{3}{2}}} \quad (1)$$

where H is magnetic field strength in unit ampere per metre (Amp / m), μ_0 is the permeability of free space, N is the number of turns, r is the radius of the coil, and x is the distance between current-element and reference point. Whenever the perpendicular H -field is penetrating a contour area of conductor plate A , it is potentially interchanged into magnetic flux density (or magnetic induction) B in unit Webber (Wb). At this time, the process of magnetization M occurs in the conductor plate which indicates the movement of atom correlated to H-field. The B equation can be written as below:

$$B = \mu_0(H + M) \tag{2}$$

where μ_0 is permeability of free space and $M = \chi H$. χ is magnetic susceptibility of conductor values is varies among diamagnetic material, paramagnetic material and ferromagnetic material. The magnetic induction is the production of electromotive force (EMF) ϵ or potential different or voltage in plate EMF. Equation is shown in equation (3).

$$\epsilon (EMF) = \frac{dB}{dt} \cos \theta \tag{3}$$

where ϵ is voltage induced, ϕ_B is magnetic flux density and $\cos \theta$ is the angle between the applied field and the given area. Proven by Faraday law, whenever the time rate of change of the B-field is induced, the potential difference in the plate has tendency to induce an electric field, E . Fig.2 shows the magnetic flux density in loop induced by the current carrying coil. Due to potential different vicinities, the E-field is moved in a circular motion around the loop. This phenomenon is known as Eddy Current.

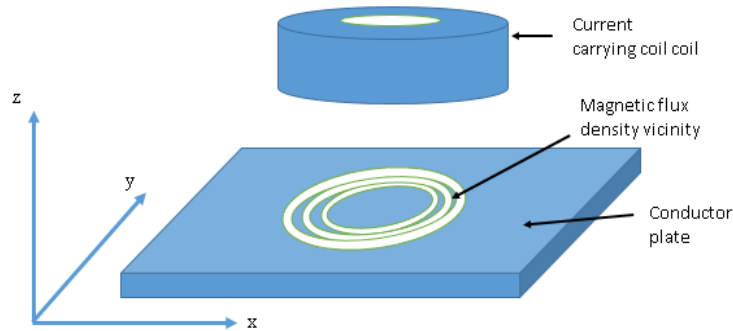


Fig. 2 - Illustration of Eddy Current [13]

The motion of Eddy Current is dependent on conductivity σ of material. The higher the σ influence the freely motion of Eddy Current charge particle in the area of conductor plate. The Eddy Current in the certain area is known as Eddy Current Density I_{CD} . At this moment, the continuous magnetic field from current-carrying coil exerts a Lorentz force F_L on I_{CD} in the plate [9]. Lorentz force is the configuration of force from magnetic force and electric force relationship as shown as equation (4):

$$F_L = I_{CD} \times H \tag{4}$$

Consequently, the current carrying coil now begin to drag and lift due to drag and lift force as shown at Fig. 3

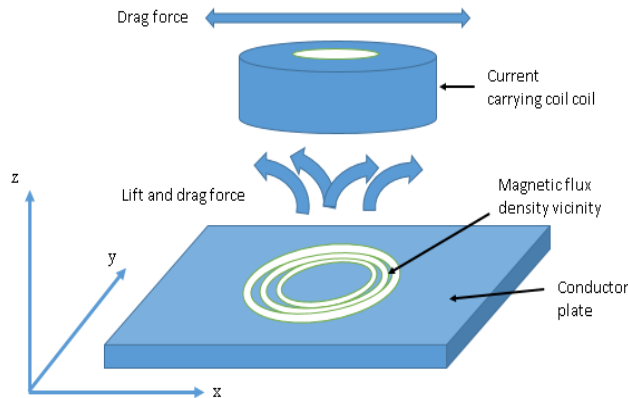


Fig. 3 - Illustration of I_{CD} with lift and drag force [9]

2.1 Thickness Effect I_{CD}

When the electrical potential is applied to the conductor, the electric current will freely flow in it. This is due to the resistivity ρ and conductivity σ that are related to the mobility of electron assessment in the conductor. The conductor with high resistivity mitigates the movement of an electron, thus reduces the electric current flow. The conductivity is reciprocal to resistivity by the equation (5):

$$\rho = \frac{1}{\sigma} \quad (5)$$

where ρ is resistivity measured in-unit Ohm while conductivity σ in unit Mho. The value of ρ is useful for identifying the overall resistance of the conductor. The relationship can be derived in equation (6) and (7):

$$R \propto \frac{l}{A} \quad (6)$$

$$R = \rho \frac{l}{A} \quad (7)$$

where R is electrical resistance, $A = a^2$ is the cross-section area of the square conductor and l is the length of the conductor or can be assumed as the length of thickness l shown in Figure 2.4. From the equation (8), the resistance of the conductor is reduced, hence enhancing the conductivity in it.

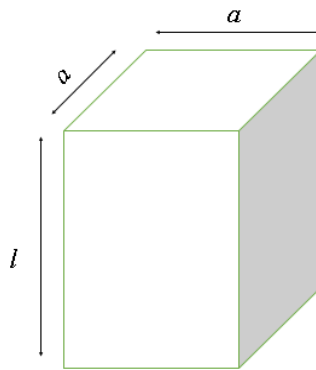


Fig. 4 - Square plate with thickness l

2.2 Frequency Effect I_{CD}

The conductor beneath the exciter coil has possibility to contribute and distribute eddy current at the conductor's surface more than an insidious area of plate conductor. This is due to skin effect phenomenon which is dependent on frequency operation f . The suitable range of frequency operation will encourage the accumulation of I_{CD} inside the conductor. The higher frequency may trigger the I_{CD} reduction exponentially from its original value at the surface according to the depth d from the surface. The relationship is in equation (8):

$$I_{CD} = I_{CD} e^{-\frac{d}{\delta}} \quad (8)$$

where δ is the skin depth which describe the I_{CD} has decline by the factor of $1 / e$ from the surface value. The skin depth formula is derived in equation (9):

$$\delta = \sqrt{\frac{2\rho}{\omega \mu_r \mu_0}} \quad (9)$$

where ρ is resistivity of conductor and $\omega = \pi f$ is angular frequency.

3. Methodology

This part discusses the step to simulate using ANSYS Maxwell Software.

- i. Choose the suitable design and method
The most preferred design is based on previous experiment and design [12].
- ii. Draw the model using a suitable software
Draw the eddy current model in 3D by using ANSYS Maxwell Electronic Desktop.
- iii. Assign materials involved
The coil is made up of copper while the plate comes with two different materials which is aluminium and copper.
- iv. Assign region and boundary of simulation
Both of specimen should be placed in an invisible closed region, by setting offset range more than 10 percent.
- v. Mesh operation
Divide the region of interest into small calculation areas. Two optional operations are given either 'on selection mesh operation' (preferred for eddy current measurement) or 'in selection mesh operation' (preferred for skin depth measurement).
- vi. Simulation
ANSYS Maxwell will perform the model-based calculation process. The result is displayed in the simulation after design. The result of the current density can be viewed from this simulation.
- vii. Post-process analysis
After simulation, these models will be analysed according to current density induction.

4. Results and Analysis

Fig. 4(a) and (b) show the complete structure of the ideal current-carrying coil over the square plate. The approximate gap distance between the coil and plate is about 1 cm. The plate thickness and width is initially 3 cm and 20 cm respectively. The coil was excited by 26A of the AC current source. All these objects are located in the closed region. To identify the I_{CD} occurred at the conductor's surface, one straight line of indicator has been drawn aligned with the y-axis.

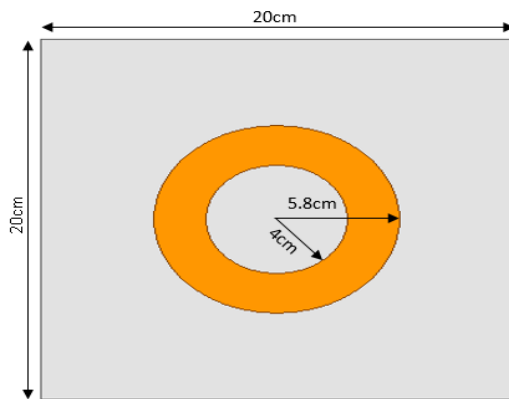


Fig. 4 - (a) Top view

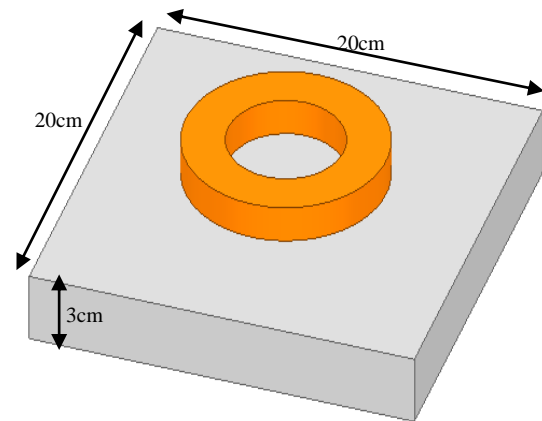


Fig. 4 - (b) Trimetric view

(a) Effect of Plate Thickness

The experiment has been done on square copper plate which has high intensity to produce more I_{CD} . A thicknesses of chopper plate are increased from 1 cm, 3 cm, 6 cm and 9 cm. Whereas, the width is set to 20 cm. The frequency of the source is still 50 Hz. Fig. 5 (a) to (d) show the I_{CD} plotted on the conductor's surface respectively to the thickness.

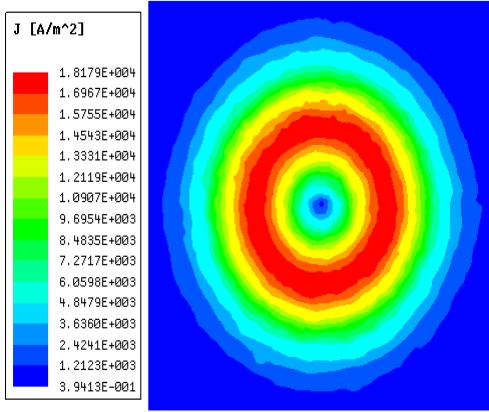


Fig. 5 - (a) I_{CD} on 1cm plate

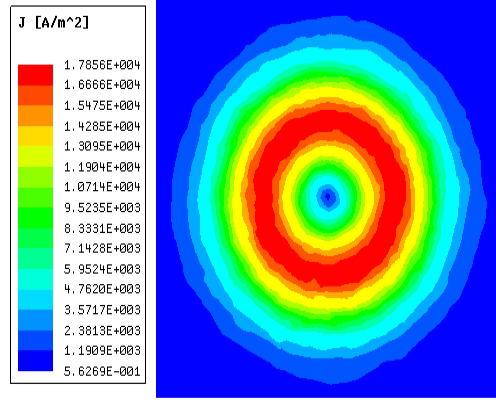


Fig. 5 - (b) I_{CD} on 3cm plate

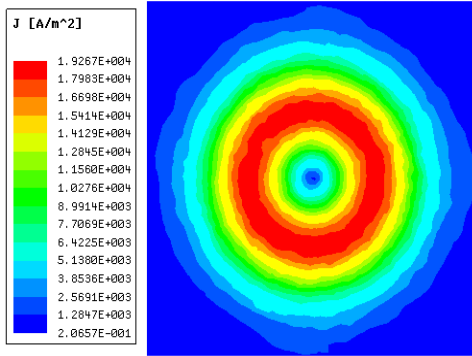


Fig. 5 - (c) I_{CD} on 6cm plate

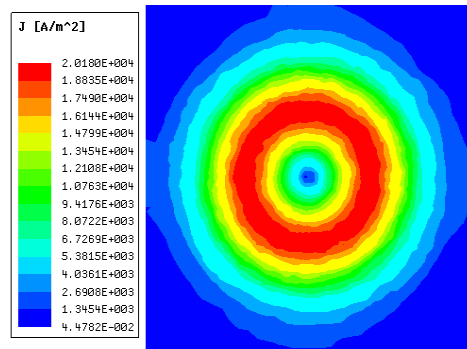


Fig. 5 - (d) I_{CD} on 9cm plate

From the result, the value of I_{CD} is increased proportionally to the thickness as shown in Fig. 6 and Table 1. The thickness is associated with the resistance of the conductor. From equation (8), whenever the thickness is increased, the resistance of the conductor becomes weaker. Low resistance produces higher conductivity, thus the formation of I_{CD} also become higher. Unpredictable results are shown when the thickness is 0 cm is due to higher eddy current loss.

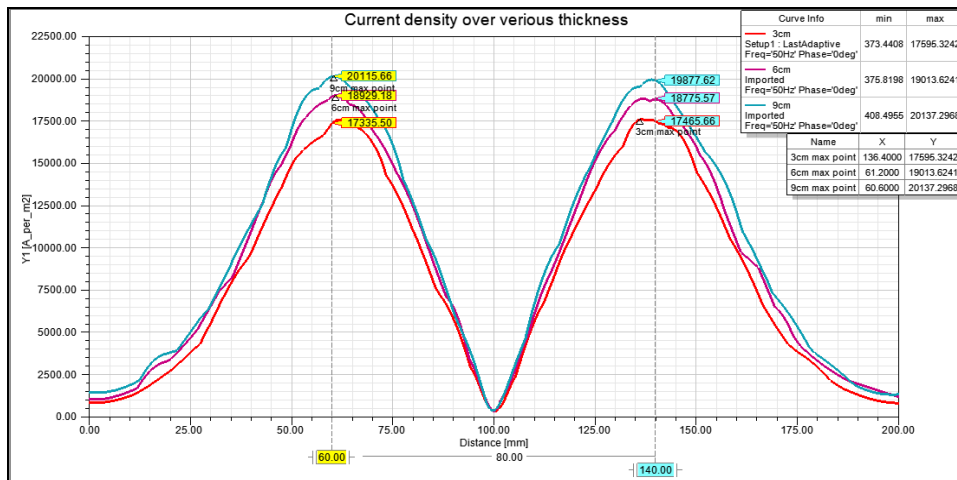


Fig. 6 - Overall I_{CD} on 3cm, 6cm, and 9cm plate thickness

Table 1 is tabulates the minimum and maximum value of I_{CD} with different thickness. Based on the results, when the thickness is 3 cm, the value is 373.44 A/mm² (min) and 17596.32 A/mm² (max) of I_{CD} respectively. Moreover, when the thickness is 9 cm, the value is increased to 408.50 A/mm² (min) and 20137.30 (max) of I_{CD} respectively. The results show that when the thickness is increase, then I_{CD} is increased to 20KA/m².

Table 1 - Comparison I_{CD} over various thickness of plate.

Thickness (cm)	I_{CD} minimum (A / m ²)	I_{CD} maximum (A / m ²)
1cm	Unclearified	Unclearified
3cm	373.44	17596.32
6cm	375.82	19013.62
9cm	408.50	20137.30

(b) Effect of Plate Frequency

The simulation has been done on copper plate which has high intensity to produce more I_{CD} . The frequency is set at 45 Hz, 50 Hz, 55 Hz, and 60 Hz. While, the plate thickness is still the same at 3 cm. Fig. 7 (a) to (d) show the I_{CD} plotted on the conductor's surface with relation to the frequency of AC source.

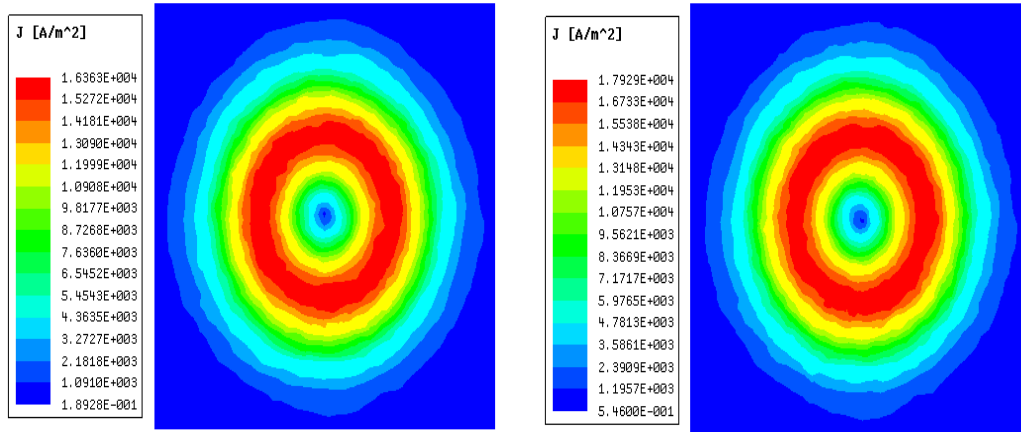


Fig. 7 - (a) I_{CD} when 45 Hz

Fig. 7 - (b) I_{CD} when 50 Hz

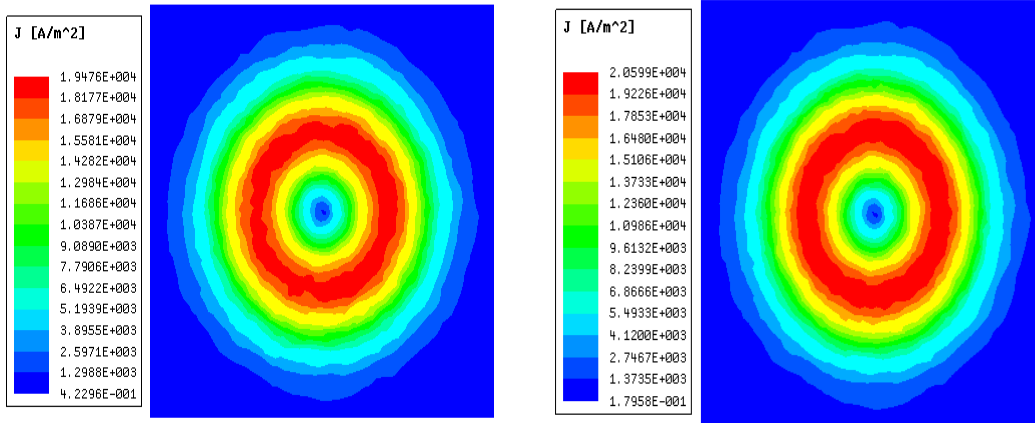


Fig. 7 - (c) I_{CD} when 55 Hz

Fig. 7 - (d) I_{CD} when 60 Hz

From Fig. 8 and Table 2, the concentration of I_{CD} mostly appear at the surface of conductor as the frequency increases. Referring to skin depth formula equation (2.9), the I_{CD} decreases with depth becoming proportional to higher frequency. It means that the initial value of I_{CD} is highly concentrated at the surface and start to decrease when it is further from the surface.

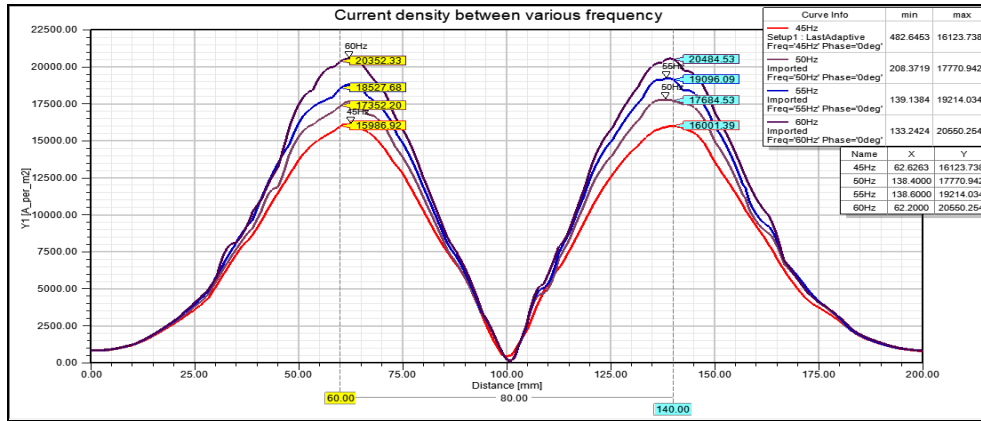


Fig. 8 - Overall I_{CD} on 45Hz, 50Hz, 55Hz and 60Hz of frequency

Table 2 tabulates the minimum and maximum value of I_{CD} with different frequency. Based on the results, when f is 45 Hz, the value is 482.65 A/mm² (min) and 16123.74 A/mm² (max) of I_{CD} respectively. Moreover, when the f is 55 Hz, the value is 139.14 A/mm² (min) and 19214.03 (max) of I_{CD} respectively. Based on the results shown, when the frequency, f is increased to 60 Hz the maximum I_{CD} is increased up to 20.55KA/m².

Table 2 - Comparison I_{CD} over various frequency

Frequency (Hz)	I_{CD} minimum(A / m ²)	I_{CD} maximum (A / m ²)
45	482.65	16123.74
50	208.37	17770.94
55	139.14	19214.03
60	133.24	20550.25

5. Conclusion

The objective has been achieved for this paper. The objectives of this research are to analyze the relationship between I_{CD} induction correlated to material thickness, and frequency source. This project uses software for simulations as data assessment. The determination of I_{CD} is made by using ANSYS Maxwell software. The project uses copper for the conductor (diamagnetic conductor). This project uses different thickness of conductor like 1 cm, 3 cm, 6 cm, and 9 cm. The project is analysed by the injection of difference frequency operation sources like 45 Hz, 50 Hz, 55 Hz, and 60 Hz from the exciter coil. Based on the simulation results, I_{CD} that is obvious at the top surface of the conductor is influenced by many factors. The factors are the type of the conductor’s material, conductor thickness, and frequency excitation. Most of the conductor with positive susceptibility and magnetic permeability properties have potential to conduct more I_{CD} according to magnetization operation. The conductor with large dimension and thickness has ability to minimize conductor’s resistance as less resistance assures the freely motion of electrons. The result also prove that maximization of I_{CD} concentration can be achieved whenever the conductor is excited by higher frequency.

References

- [1] Nordin N. H., Masirin M. I. M., Ghazali I. and Azis M. I. (2017) Appraisal on Rail Transit Development: A Review on Train Service and Safety, IOP Conference Series: Materials Science and Engineering, 226
- [2] Lee H. W., Kim K. C. and Lee J. (2006) Review of Maglev Train Technologies, IEEE Transactions on Magnetics, 42, 1917-1925
- [3] Emil C. (2006) Permanent Magnet Levitation Stabilized by Diamagnetic Material: A case-study. 6th International Conference on Computational Electromagnetics, 1-2
- [4] Witzel J. (2010) Magnetic levitation [My Favored Experiment], IEEE Instrumentation & Measurement Magazine, 13, 39-41
- [5] Janousek L., Capova K., Yusa N and Miya K. (2008) Multiprobe Inspection for Enhancing Sizing Ability in Eddy Current Non-destructive Testing, IEEE Transactions on Magnetics, 44, 1618-1621
- [6] Livingston J. D. (2011) Rising Force. The Magic of Magnetic Levitation, Harvard University Press, 78-80
- [7] Gulbahce M. O., Kocabas D. A. and Atalay A. K. (2013) A study to determine the act of excitation current on braking torque for a low power eddy current brake, IEEE International Electric Machines & Drives Conference (IEMDC)

- [8] Jayawant B. V. (1982) Electromagnetic suspension and levitation, IEE Proceedings A - Physical Science, Measurement and Instrumentation, Management and Education – Reviews, 129, 549-581
- [9] Thompson M. T. (2000) Eddy current magnetic levitation. Models and experiments, IEEE Potentials. 19, 40-44.
- [10] Buckley J. M. (2003) An introduction to eddy current testing theory and technology, 8, 7
- [11] Sweetnam R. T. (2013) Microscopic origins of diamagnetic, ferromagnetic and paramagnetic magnetization. 1st Annual Active and Passive RF Devices Seminar, Glasgow, 41-42
- [12] Yaqin L., Pingan D. and Yating Y. (2006) 3D Modeling and Simulation of the Electromagnetic Field in Eddy Current Sensor, IEEE International Conference on Industrial Technology, Mumbai, 1149-1153
- [13] Tang D D. and Lee Y. J. (2010) Magnetic Memory - Fundamentals and Technology, Cambridge University Press, 1-3